



Article

Tolstykite, $\text{Au}_3\text{S}_4\text{Te}_6$, a new mineral from Maletoyvayam deposit, Kamchatka peninsula, Russia

Anatoly V. Kasatkin^{1*} , Fabrizio Nestola², Jakub Plášil³, Jiří Sejkora⁴, Anna Vymazalová⁵ and Radek Škoda⁶

¹Fersman Mineralogical Museum of the Russian Academy of Sciences, Leninsky Prospekt 18-2, 119071 Moscow, Russia; ²Dipartimento di Geoscienze, Università di Padova, Via Gradenigo 6, I-35131, Padova, Italy; ³Institute of Physics of the CAS, Na Slovance 1999/2, 18221 Praha 8, Czech Republic; ⁴Department of Mineralogy and Petrology, National Museum, Cirkusová 1740, 193 00 Prague 9, Czech Republic; ⁵Czech Geological Survey, Geologická 6, 152 00 Prague 5, Czech Republic and ⁶Department of Geological Sciences, Faculty of Science, Masaryk University, Kotlářská 2, 611 37, Brno, Czech Republic

Abstract

Tolstykite, ideally $\text{Au}_3\text{S}_4\text{Te}_6$, is a new mineral from the Gaching ore occurrence of the Maletoyvayam deposit, Kamchatka peninsula, Russia. It occurs as individual anhedral grains up to 0.05 mm or as intergrowths with native Se, native Te and tripuhyite. Other associated minerals include calaverite, fischesserite, Cu–Te-rich ‘fahlores’ [stibiogoldfieldite, ‘arsenogoldfieldite’, tennantite-(Cu), tetrahedrite-(Zn)], galena, gold, maletoyvayamite, minerals of famatinite–luzonite series, pyrite, baryte, ilmenite, magnetite, quartz and V-bearing rutile. Tolstykite is bluish-grey, opaque with metallic lustre and grey streak. It is brittle and has an uneven fracture. Cleavage is good on {010} and {001}. $D_{\text{calc}} = 7.347 \text{ g/cm}^3$. In reflected light, tolstykite is grey with a bluish shade. No birefractance, pleochroism and internal reflections are observed. In crossed polars, it is weakly anisotropic with bluish to brownish rotation tints. The reflectance values for wavelengths recommended by the Commission on Ore Mineralogy of the International Mineralogical Association are ($R_{\text{min}}/R_{\text{max}}$, %): 32.6/34.3 (470 nm), 32.4/34.1 (546 nm), 32.6/34.5 (589 nm) and 33.0/35.0 (650 nm). The Raman spectrum of tolstykite contains the main bands at 297, 203, 181, 151 and 127 cm^{-1} . The empirical formula calculated on the basis of 13 atoms per formula unit is $(\text{Au}_{2.98}\text{Ag}_{0.01})_{\Sigma 2.99}(\text{S}_{3.59}\text{Se}_{0.41})_{\Sigma 4.00}\text{Te}_{6.01}$. Tolstykite is triclinic, space group $P\bar{1}$, $a = 8.977(5)$, $b = 9.023(2)$, $c = 9.342(6) \text{ \AA}$, $\alpha = 94.03(3)$, $\beta = 110.03(3)$, $\gamma = 104.27(4)^\circ$, $V = 679.0(3) \text{ \AA}^3$ and $Z = 2$. The strongest lines of the powder X-ray diffraction (XRD) pattern [d , Å (I , %) (hkl)] are: 8.59 (18) (010); 2.90 (100) (0 $\bar{1}$ 3); 2.23 (13) (133); 1.89 (21) (134). Tolstykite is the S-analogue of maletoyvayamite, $\text{Au}_3\text{Se}_4\text{Te}_6$. The structural identity between them is confirmed by powder XRD and Raman spectroscopy. The mineral honours Russian mineralogist Dr. Nadezhda Dmitrievna Tolstyk for her contributions to the mineralogy of gold and platinum-group elements and the study of ore deposits.

Keywords: tolstykite, new mineral, chemical composition, powder X-ray diffraction, maletoyvayamite, Maletoyvayam deposit, Kamchatka peninsula

(Received 18 July 2022; accepted 3 September 2022; Accepted Manuscript published online: 19 September 2022; Associate Editor: Owen Missen)

Introduction

The synthetic gold chalcogenides of the Au–Te–Se–S system are the long-standing subject of numerous studies in experimental mineralogy (see, e.g. Cranton and Heyding, 1968; Ettema *et al.*, 1994; Ishikawa *et al.*, 1995; Wang, 2000; Concepción Gimeno and Laguna, 2008; Ciesielski *et al.*, 2019; Palyanova *et al.*, 2019, 2020 *et al.*). However, naturally occurring phases of this system remained unknown until recent times when two new minerals, maletoyvayamite, $\text{Au}_3\text{Se}_4\text{Te}_6$ (Tolstyk *et al.*, 2020), and gachingite, $\text{Au}(\text{Te}_{1-x}\text{Se}_x)$, $0.2 \approx x \leq 0.5$ (Tolstyk *et al.*, 2022), were discovered at the Gaching ore occurrence of the Maletoyvayam deposit, Kamchatka peninsula, the Far East of the Russian Federation. Their formation was possible due to the very special conditions requiring an abundant source of Au, S, Se and Te and a strongly oxidising environment (Tolstyk *et al.*, 2018).

Herein, we provide the description for the third mineral of the above system from the same occurrence that we named tolstykite (pronounced: tol sty khait; cyrilic – толстyxит) in honour of Russian mineralogist Dr. Nadezhda Dmitrievna Tolstyk (Надежда Дмитриевна Толстyx), born October 7th, 1954, for her contributions to the mineralogy of gold and platinum-group elements (PGE) and the study of ore deposits. Dr. Tolstyk is the leading researcher at the Sobolev Institute of Geology and Mineralogy, Novosibirsk, Russia and the author of numerous publications focused on the mineralogy, geology and geochemistry of noble minerals (see, e.g. Tolstyk *et al.*, 2008, 2009, 2018, 2019, 2020, 2021). In addition, she is the discoverer and author of several noble minerals, including maletoyvayamite and gachingite mentioned above.

The new mineral and its name (symbol Tls) have been approved by the Commission on New Minerals, Nomenclature and Classification of the International Mineralogical Association (IMA2022-007; Kasatkin *et al.*, 2022). The holotype specimen is deposited in the collections of the Fersman Mineralogical Museum of the Russian Academy of Sciences, Moscow, Russia, with the registration number 5795/1.

*Author for correspondence: Anatoly V. Kasatkin, Email: anatoly.kasatkin@gmail.com
Cite this article: Kasatkin A.V., Nestola F., Plášil J., Sejkora J., Vymazalová A. and Škoda R. (2023) Tolstykite, $\text{Au}_3\text{S}_4\text{Te}_6$, a new mineral from Maletoyvayam deposit, Kamchatka peninsula, Russia. *Mineralogical Magazine* 87, 34–39. <https://doi.org/10.1180/mgm.2022.109>

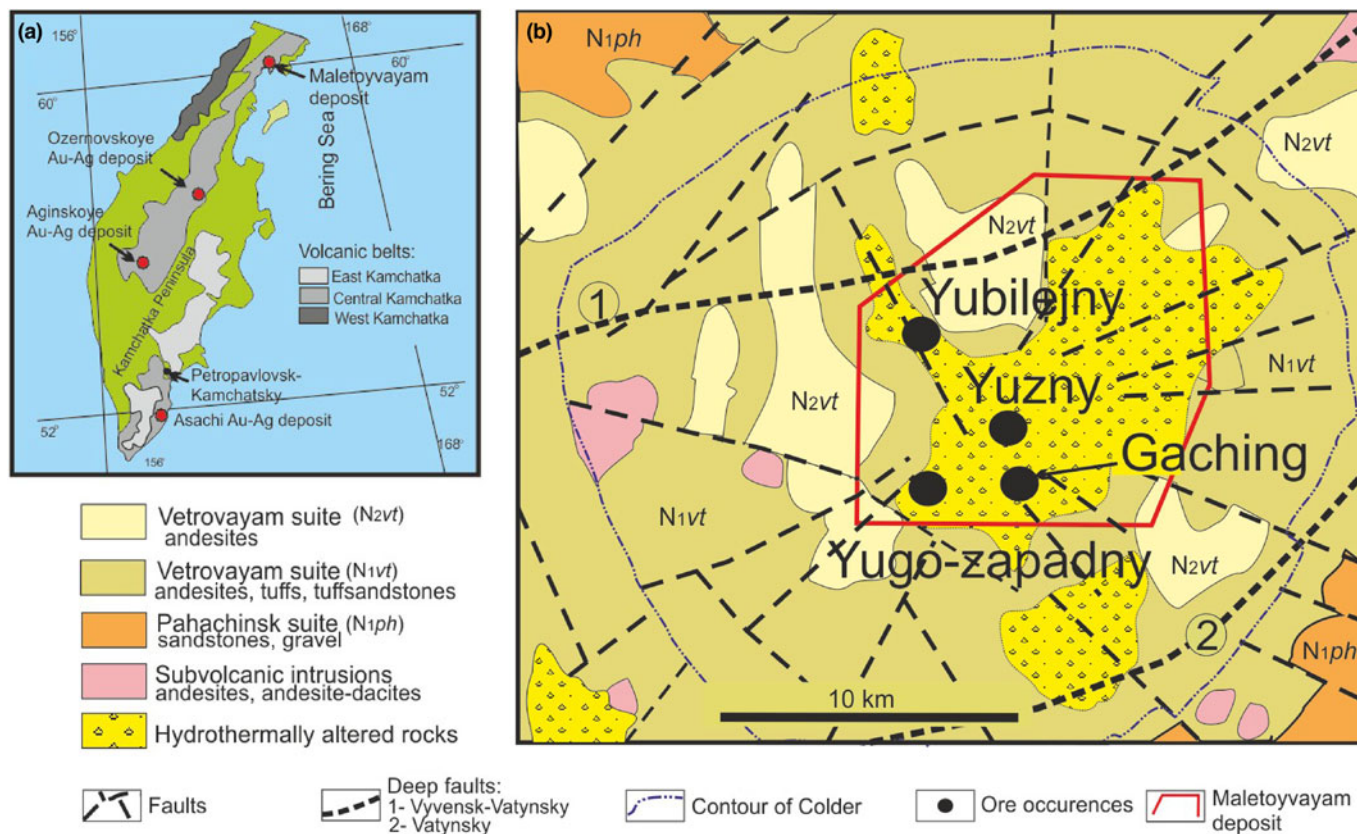


Fig. 1. Geographic and geological position of the Maletoyvayam deposit: (a) volcanic belts and epithermal deposits of Kamchatka peninsula including Maletoyvayam; (b) geological map of the Maletoyvayam deposit (modified after Sidorov *et al.*, 2020 and Tolstykh *et al.*, 2020).

Occurrence and mineral association

The Maletoyvayam deposit is located in the southwestern part of the Koryak Highland of the Central Kamchatka volcanic belt, in the Far East of the Russian Federation (60°19'51.87"N, 164°46'25.65"E). The Eocene–Oligocene Central Kamchatka volcanic belt is ~1800 km long. It is controlled by the Main Kamchatka deep fault, displaying many gold–silver epithermal deposits, including Maletoyvayam (Fig. 1a). The latter is particularly confined to a volcano-tectonic structure (up to 30 km) within the Vetrovayam volcanic zone located in the northeastern region of the Central Kamchatka volcanic belt and limited by the Koryak Highland in the southwestern part (Fig. 1b). This whole structure is controlled by the Vyvenskiy northeast-striking deep fault and the northwest-striking faults zone. Stratified subvolcanic and intrusive formations, as well as Quaternary sediments, are the main elements of the ore field (Sidorov *et al.*, 2020).

Unlike other epithermal deposits of the Central Kamchatka volcanic belt, which belong to the low-sulfidation type, the Maletoyvayam deposit is assigned to the high-sulfide one (Sidorov *et al.*, 2020; Tolstykh *et al.*, 2018, 2020, 2022). The Maletoyvayam deposit is composed of andesites, tuffs and tuffaceous sandstones. The main gangue minerals are quartz, alunite, native sulphur and kaolinite. The main ore minerals include pyrite and gold. A detailed description of the Maletoyvayam deposit, its geology, geochemical features and mineralisation can be found elsewhere (Kalinin *et al.*, 2012; Shapovalova *et al.*, 2019; Sidorov *et al.*, 2020; Tolstykh *et al.*, 2018, 2020, 2022).

The Maletoyvayam deposit comprises four ore occurrences: Yubileyniy, Yugo-Zapadniy, Tyulul and Gaching. The latter is located at the head of the Gachingalhovayam River and differs from the others by having a significant mineral variety. Tolstykhite described in this paper is associated with calaverite, fischerite, Cu–Te-rich 'fahlores' [stibiogoldfieldite, 'arsenogoldfieldite', tennantite-(Cu) and tetrahedrite-(Zn)], galena, gold, maletoyvayamite, famatinite–luzonite series minerals, native Se, native Te, pyrite, baryte, ilmenite, magnetite, quartz, V-bearing rutile and tripuhyite.

General appearance and physical properties

Tolstykhite was found in polished sections containing a heavy-mineral concentrate from the Gaching occurrence prepared following Tolstykh *et al.* (2022). It occurs as individual anhedral grains up to 0.05 mm. Some grains of tolstykhite form intergrowths with native Se, native Te and tripuhyite, or contain tiny (<0.01 mm) inclusions of the minerals of famatinite–luzonite series and different fahlores (Figs 2a,b).

Tolstykhite is bluish-grey, opaque, with metallic lustre and a grey streak. Its tenacity is brittle and its fracture is uneven. Cleavage is good on {010} and {001}. No parting is observed. The density calculated using the empirical formula and unit-cell volume obtained from powder XRD data is 7.347 g/cm³. In reflected light, tolstykhite is grey with a bluish shade. No birefringence, pleochroism and internal reflections are observed. In crossed polars, it is weakly anisotropic with bluish to brownish

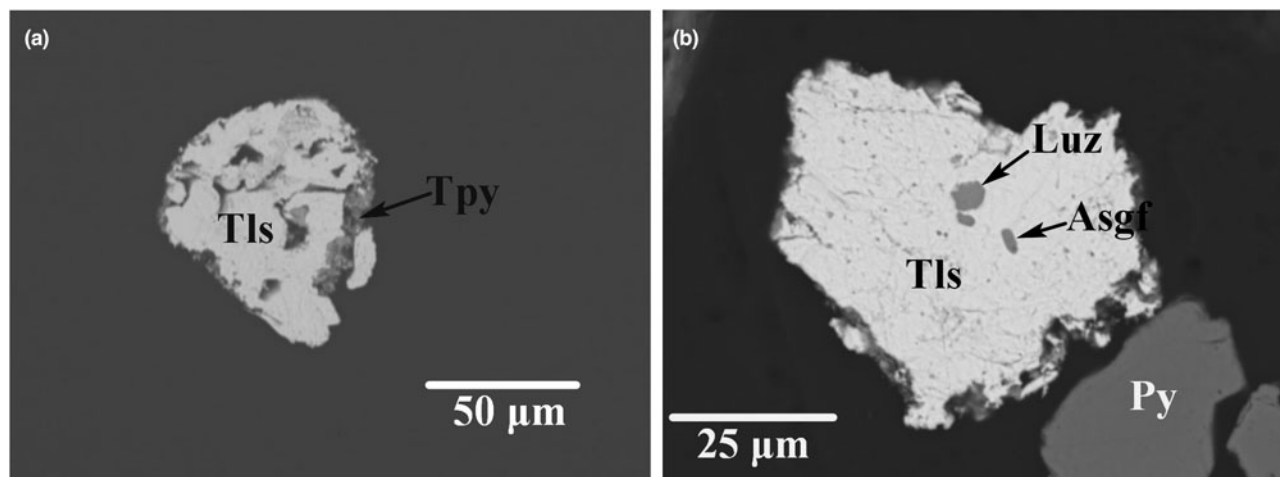


Fig. 2. Anhedral grains of tolstykhite (Tls): (a) intergrown with tripuhyite (Tpy); (b) with small inclusions of luzonite (Luz) and ‘arsenogoldfieldite’ (Asgf) in association with pyrite (Py). Polished section. Back-scattered electron image, sample no. 880T.

rotation tints. The reflectance values were measured in the air relative to a WTiC standard using a Zeiss 370 spectrophotometer MSP400 TIDAS mounted to Leica microscope with a 100× objective (National Museum in Prague, Czech Republic). Data are given in Table 1 and plotted in Fig. 3 in comparison with the published data for maletoyvayamite (Tolstykh *et al.*, 2020).

Raman spectroscopy

The Raman spectrum of tolstykhite (Fig. 4) was collected in the range 80–4000 cm^{-1} using a DXR dispersive Raman Spectrometer (Thermo Scientific) mounted on a confocal Olympus microscope (National Museum in Prague, Czech Republic). The Raman signal was excited by an unpolarised 633 nm He–Ne gas laser and detected by a CCD detector (size 1650 × 200 pixels, Peltier-cooled to -60°C , quantum efficiency 50% and dynamic range 360–1100 nm). The experimental parameters were: 100× objective, 10 s exposure time, accumulation of 100 exposures, 50 μm pinhole spectrograph aperture and 0.5 mW laser power level. The spectra were repeatedly acquired from different grains in order to obtain a representative spectrum with the best signal-to-noise ratio. The possible thermal damage of the measured point was excluded and assessed by visual inspection of the exposed surface after measurement, observation of possible decay of spectral features at the start of excitation, and checking for thermal downshift of Raman lines. The instrument was set

up by a software-controlled calibration procedure using multiple neon emission lines (wavelength calibration), multiple polystyrene Raman bands (laser-frequency calibration) and standardised white-light sources (intensity calibration). Spectral manipulations were performed using *Omnic 9* software (Thermo Scientific).

The main bands observed in the spectrum are (in wavenumbers): 297, 203, 181, 151 and 127 cm^{-1} that are close to Raman spectra provided for natural ‘S-maletoyvayamite’ with the composition $\text{Au}_3\text{Te}_6(\text{S}_{3.4}\text{Se}_{0.6})_{\Sigma 4.0}$ and synthetic $\text{Au}_{2.92}\text{Te}_{6.13}(\text{S}_{2.15}\text{Se}_{1.80})_{\Sigma 3.95}$ (Palyanova *et al.*, 2022) as well as for maletoyvayamite $\text{Au}_3\text{Se}_4\text{Te}_6$ (the Se-analogue of tolstykhite) and its synthetic analogue (Tolstykh *et al.*, 2020; Palyanova *et al.*, 2022). The strong bands at 127 and 151 cm^{-1} in tolstykhite could be tentatively assigned to Au–Te bonds whereas the ones at 181, 297 and the shoulder at 203 cm^{-1} – to Au–S bonds. According to Palyanova *et al.* (2022), the band in the 280–290 cm^{-1} range appears when chemical analyses show the presence of S substituting for Se, and the more S is present in the sample, the stronger the corresponding band is. This is in line with the sharp peak of 297 cm^{-1} in tolstykhite, which is absent in maletoyvayamite and synthetic $\text{Au}_3\text{Se}_4\text{Te}_6$. Also, in comparison with published peaks for maletoyvayamite (178, 158, 137 and 101 cm^{-1} – Tolstykh *et al.*, 2020), some observed bands of tolstykhite are shifted to higher

Table 1. Reflectance data of tolstykhite.*

| λ (nm) | R_{\min} (%) | R_{\max} (%) | λ (nm) | R_{\min} (%) | R_{\max} (%) |
|----------------|----------------|----------------|----------------|----------------|----------------|
| 400 | 30.5 | 30.5 | 560 | 32.5 | 34.3 |
| 420 | 32.1 | 32.9 | 580 | 32.6 | 34.4 |
| 440 | 32.6 | 34.0 | 589 | 32.6 | 34.5 |
| 460 | 32.6 | 34.4 | 600 | 32.7 | 34.7 |
| 470 | 32.6 | 34.3 | 620 | 32.9 | 34.9 |
| 480 | 32.5 | 34.2 | 640 | 33.0 | 35.0 |
| 500 | 32.4 | 34.0 | 650 | 33.0 | 35.0 |
| 520 | 32.4 | 34.0 | 660 | 32.9 | 34.9 |
| 540 | 32.4 | 34.1 | 680 | 33.1 | 34.9 |
| 546 | 32.4 | 34.1 | 700 | 33.1 | 34.8 |

*The values required by the Commission on Ore Mineralogy are given in bold.

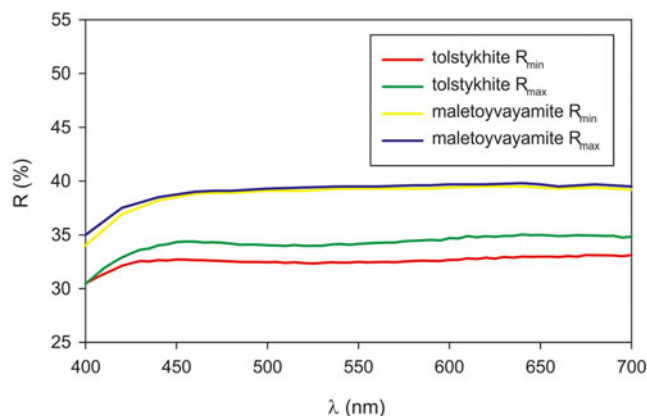


Fig. 3. Reflectivity curves for tolstykhite compared with published data for maletoyvayamite (Tolstykh *et al.*, 2020).

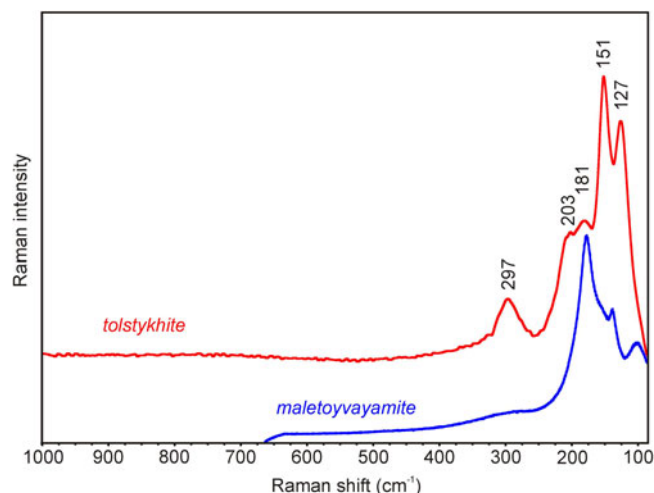


Fig. 4. Raman spectrum of tolstykhite in comparison with maletoyvayamite (taken from Tolstykh *et al.*, 2020).

wavenumbers (Fig. 4). These shifts are probably also connected with the S–Se substitution, as Hooke's Law predicts (Nakamoto, 1986). Analogous shifts have been reported as a consequence of S–Se substitution in permingeatite–famatinite/luzonite (Škácha *et al.*, 2014), tetrahedrite/hakite (Škácha *et al.*, 2017) or chalcostibite/příbramite (Sejkora *et al.*, 2018).

Chemical composition

Seven electron-microprobe analyses were carried out with a Cameca SX-100 electron microprobe (wavelength dispersive spectroscopy mode with an accelerating voltage of 25 kV, a beam current on the specimen of 10 nA and a beam diameter of 1 μm) at the Department of Geological Sciences, Faculty of Science, Masaryk University, Brno, Czech Republic. Peak counting times (CT) were 20 s for all elements; CT for each background was one-half of the peak time. Matrix correction by PAP software (Pouchou and Pichoir, 1985) was applied to the data.

Analytical data and used standards are given in Table 2. Contents of other elements with atomic numbers higher than that of beryllium are below detection limits. The empirical formula based on 13 atoms per formula unit is $(\text{Au}_{2.98}\text{Ag}_{0.01})_{\Sigma 2.99}(\text{S}_{3.59}\text{Se}_{0.41})_{\Sigma 4.00}\text{Te}_{6.01}$. The ideal chemical formula is $\text{Au}_3\text{S}_4\text{Te}_6$ which requires Au 39.79, S 8.64, Te 51.57, a total of 100 wt.%.

X-ray diffraction data

Single-crystal XRD studies could not be carried out because of the absence of single crystals: grains of tolstykhite are cryptocrystalline and inhomogeneous (see Fig. 5 showing diffraction rings

Table 2. Chemical composition of tolstykhite (wt.%).

| Constituent | Wt.% | Range | S.D. | Probe standard |
|-------------|-------|-------------|------|----------------|
| Ag | 0.10 | 0.04–0.18 | 0.05 | Ag |
| Au | 38.75 | 38.22–39.60 | 0.53 | Au |
| S | 7.60 | 6.76–8.24 | 0.60 | chalcopyrite |
| Se | 2.15 | 1.83–2.60 | 0.31 | PbSe |
| Te | 50.66 | 50.40–51.26 | 0.37 | HgTe |
| Total | 99.26 | | | |

S.D. – standard deviation

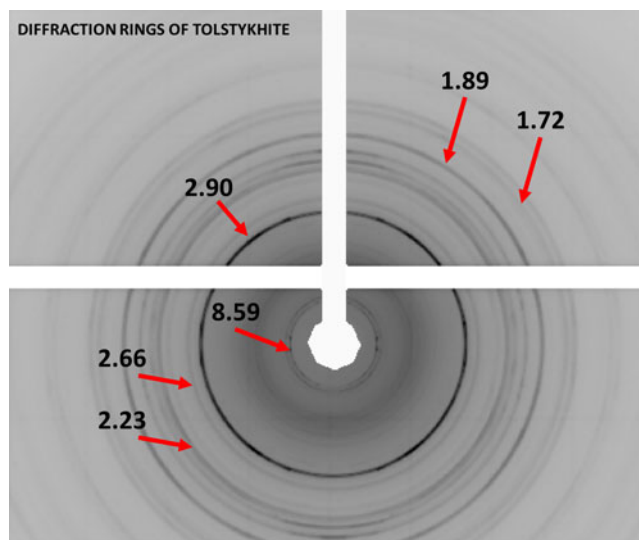


Fig. 5. Diffraction rings of tolstykhite.

typical of polycrystalline materials). Thus, an irregular aggregate not larger than 50 μm was collected in powder diffraction mode using a Supernova single-crystal X-ray Rigaku-Oxford Diffraction diffractometer equipped with a Pilatus 200 K Dectris detector and an X-ray micro-source (MoK α radiation) with a spot size of ~ 0.12 mm (University of Padova, Italy). The detector-to-sample distance was 68 mm. A standard phi scan mode as implemented in the powder power tool of *CrysAlisPro* was used for the powder data collection. We collected 360 frames, 1° and 120 seconds of exposure per frame for a total of ~ 12 hours of data collection. The observed d spacings are reported in Table 3. From these data, the unit-cell parameters of tolstykhite were obtained and gave the following values: triclinic, $P\bar{1}$, $a = 8.976(5)$, $b = 9.030(2)$, $c = 9.343(5)$ Å, $\alpha = 93.97(3)$, $\beta = 110.02(3)$, $\gamma = 104.38(4)^\circ$, $V = 679.2(3)$ Å³ and $Z = 2$.

Crystal structure and relation to other minerals

We assume that tolstykhite is isotypic with maletoyvayamite, with sulfur in the former substituting for selenium in the latter. A comparison of powder XRD for tolstykhite and maletoyvayamite (Table 3) demonstrates the structural identity between these two minerals. For their further comparison, see Table 4.

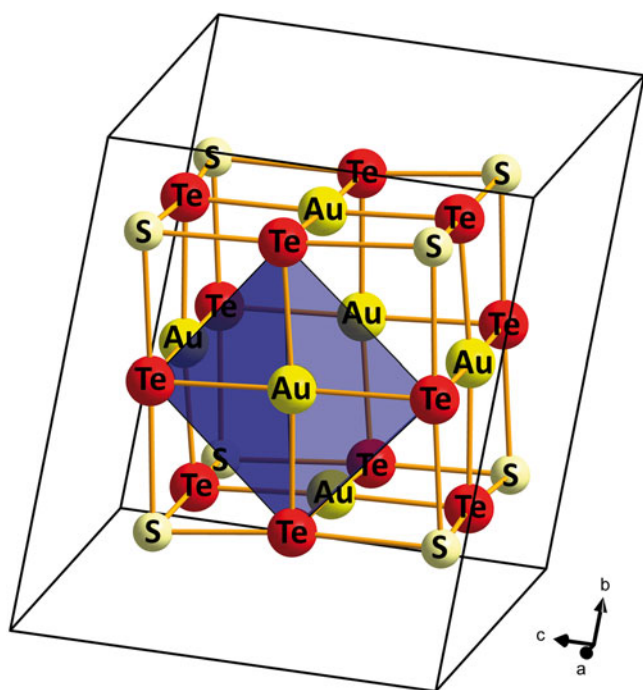
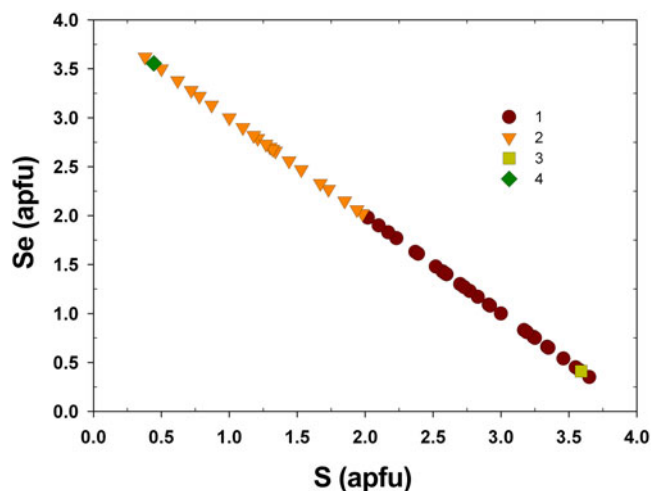
Table 3. Comparison of powder XRD patterns (d in Å) of tolstykhite and maletoyvayamite (Tolstykh *et al.*, 2020)

| Tolstykhite | | | | Maletoyvayamite | |
|------------------|------------------|-------------------|---------------|------------------|------------------|
| l_{obs} | d_{obs} | d_{calc} | hkl | l_{obs} | d_{obs} |
| 18 | 8.59 | 8.62 | 010 | 25 | 8.65 |
| 3 | 3.76 | 3.72 | 20 $\bar{2}$ | 1 | 3.72 |
| 100 | 2.90 | 2.89 | 0 $\bar{1}$ 3 | 100 | 2.91 |
| 6 | 2.66 | 2.69 | 2 $\bar{3}$ 1 | 3 | 2.62 |
| 3 | 2.35 | 2.36 | 3 $\bar{3}$ 1 | 3 | 2.28 |
| 13 | 2.23 | 2.23 | 13 $\bar{3}$ | 7 | 2.22 |
| 9 | 2.14 | 2.16 | 040 | 6 | 2.18 |
| 9 | 2.03 | 2.04 | 3 $\bar{2}$ 2 | 3 | 2.07 |
| 21 | 1.89 | 1.90 | 13 $\bar{4}$ | 8 | 1.93 |
| 1 | 1.82 | 1.82 | 33 $\bar{1}$ | 8 | 1.90 |
| 7 | 1.72 | 1.71 | 240 | 6 | 1.73 |

Table 4. Comparative data for tolstykhite and maletoyvayamite.

| Mineral | Tolstykhite | Maletoyvayamite |
|---|---|--|
| End-member formula | Au ₃ S ₄ Te ₆ | Au ₃ Se ₄ Te ₆ |
| Empirical formula | Au _{2.98} Ag _{0.01} S _{3.59} Se _{0.41} Te _{6.01} | Au _{2.90} Se _{3.52} S _{0.44} Te _{6.14} |
| Colour | bluish-grey | grey |
| Lustre | metallic | metallic |
| Tenacity | brittle | brittle |
| Cleavage | good on {010} and {001} | good on {010} and {001} |
| Crystal system | Triclinic | Triclinic |
| Space group | $P\bar{1}$ | $P\bar{1}$ |
| <i>a</i> (Å) | 8.976(5) | 8.901(2) |
| <i>b</i> (Å) | 9.030(2) | 9.0451(14) |
| <i>c</i> (Å) | 9.343(5) | 9.265(4) |
| α (°) | 93.97(3) | 97.66(3) |
| β (°) | 110.02(3) | 106.70(2) |
| γ (°) | 104.38(4) | 101.399(14) |
| <i>V</i> (Å ³) | 679.2(3) | 685.9(4) |
| <i>Z</i> | 2 | 2 |
| COM reflectance values (<i>R</i> _{min} , <i>R</i> _{max} in %): | | |
| 470 nm | 32.6, 34.3 | 38.9, 39.1 |
| 546 nm | 32.4, 34.1 | 39.3, 39.5 |
| 589 nm | 32.6, 34.5 | 39.3, 39.6 |
| 650 nm | 33.0, 35.0 | 39.4, 39.7 |
| Source | This study | Tolstykh et al. (2020) |

The structure of maletoyvayamite has been solved for its synthetic analogue and reported by Tolstykh et al. (2020). The crystal structure of the synthetic analogue of maletoyvayamite contains three Au, six Te and four Se atoms in the asymmetric unit; Se atoms are replaced by the S atoms in tolstykhite (Fig. 6). The SSe₋₁ substitution is connected with the decrease in unit-cell volume, resulting from the smaller ionic radius of S compared to Se (Shannon, 1976). This decrease is noted in tolstykhite as compared with maletoyvayamite [679.2(3) vs. 685.9(4) Å³—see Table 4] and is even more apparent—in contrast with the

**Fig. 6.** Crystal structure of tolstykhite, based on the analogy with synthetic Au₃Se₄Te₆, showing the [Au₆Se₆Te₁₂] cluster. The [AuTe₄] square is emphasised.**Fig. 7.** S vs. Se in tolstykhite–maletoyvayamite series. 1 – tolstykhite; 2 – maletoyvayamite; 3 – tolstykhite holotype; 4 – maletoyvayamite holotype (1–3: our data, 4: Tolstykh, 2020).

synthetic Au₃Se₄Te₆ [679.2(3) vs. 698.81(6) Å³—see Tolstykh et al., 2020].

Our analyses show a large degree of isomorphic substitution of S for Se in the tolstykhite–maletoyvayamite pair leading to a solid-solution series from S-richest and Se-poorest tolstykhite with S_{3.65}Se_{0.35} through many intermediate members, including those corresponding to the middle of the series, to S-poorest and Se-richest maletoyvayamite with S_{0.38}Se_{3.62} (Fig. 7). Even if the structures of both minerals are not solved by direct methods, the possible ordering of S and Se in them seems highly improbable. The similarity in the radii of Se²⁻ and S²⁻ anions lead to their substitution in solid solutions of many related minerals and synthetic compounds. No cases of their ordering are known to date. Aguilarite, the only mineral whose official IMA formula, Ag₄SeS, indicates possible S–Se ordering, was, in fact, redescribed as the Se-analogue of acanthite and its structure determination revealed no ordering at room temperature (Bindi and Pingitore, 2013).

Acknowledgements. We thank Associate Editor Owen Missen, Structure Editor Oleg Siidra, two anonymous reviewers and Principal Editor Stuart Mills for valuable comments. This research was supported by the Ministry of Culture of the Czech Republic (long-term project DKRVO 2019-2023/1.II.d; National Museum, 00023272 for J.S.) and the Grant Agency of the Czech Republic (project No. 22-26485S to A.V.).

Competing interests. The authors declare none.

References

- Bindi L. and Pingitore N.E. (2013) On the symmetry and crystal structure of aguilarite, Ag₄SeS. *Mineralogical Magazine*, **77**, 21–31.
- Ciesielski A., Skowronski L., Trzcinski M., Górecka E., Pacuski W. and Szoplík T. (2019) Interaction of Te and Se interlayers with Ag or Au nanofilms in sandwich structures. *Beilstein Journal of Nanotechnology*, **10**, 238–246.
- Concepción Gimeno M. and Laguna A. (2008) Chalcogenide centred gold complexes. *Chemical Society Reviews*, **37**, 1952–1966.
- Cranton G.E. and Heyding R.D. (1968) The gold/selenium system and some gold selenotellurides. *Canadian Journal of Chemistry*, **46**, 2637–2640.
- Ettema A.R.H.F., Stegink T.A. and Haas C. (1994) The valence of Au in AuTe₂ and AuSe studied by x-ray absorption spectroscopy. *Solid State Communications*, **90**, 211–213.

- Ishikawa K., Isonaga T., Wakita S. and Suzuki Y. (1995) Structure and electrical properties of Au_2S . *Solid State Ionics*, **79**, 60–66.
- Kalinin K.B., Andreeva E.D. and Yablokova D.A. (2012) Textures and structures of Jubilee ore occurrence (Maletoyvayam ore field). Pp. 39–48 in: *Materials XI Regional youth scientific conference "The Natural Environment of Kamchatka"*. Petropavlovsk-Kamchatsky, Russia [in Russian].
- Kasatkin A.V., Nestola F., Plášil J., Sejkora J., Vymazalová A. and Škoda R. (2022) Tolstykhite, IMA 2022-007, in: CNMNC Newsletter 67. *Mineralogical Magazine*, **86**, 849–853.
- Nakamoto K. (1986) *Infrared and Raman Spectra of Inorganic and Coordination Compounds*; John Wiley and Sons: New York, USA.
- Palyanova G.A., Tolstykh N.D., Zinina V.Yu., Kokh K.A., Seryotkin Yu.V. and Bortnikov N.S. (2019) Synthetic gold chalcogenides in the Au–Te–Se–S system and their natural analogs. *Doklady Earth Sciences*, **487**, 929–934 [in Russian].
- Palyanova G., Mikhlín Y., Zinina V., Kokh K., Seryotkin Y. and Zhuravkova T. (2020) New gold chalcogenides in the Au–Te–Se–S system. *Journal of Physics and Chemistry of Solids*, **138**, 109276.
- Palyanova G., Beliaeva T., Kokh K., Seriotkin Y., Moroz T. and Tolstykh N. (2022) Characterization of synthetic and natural gold chalcogenides by electron microprobe analysis, X-ray powder diffraction, and Raman spectroscopic methods. *Journal of Raman Spectroscopy*, **53**, 1012–1022.
- Pouchou J.L. and Pichoir F. (1985) "PAP" ($\varphi\rho Z$) procedure for improved quantitative microanalysis. Pp. 104–106 in: *Microbeam Analysis* (J.T. Armstrong, editor). San Francisco Press, San Francisco.
- Sejkora J., Buixaderas E., Škácha P. and Plášil J. (2018) Micro-Raman spectroscopy of natural members along $CuSbS_2$ – $CuSbSe_2$ join. *Journal of Raman Spectroscopy*, **49**, 1364–1372.
- Shannon R.D. (1976) Revised effective ionic radii and systematic studies of interatomic distances in halides and chalcogenides. *Acta Crystallographica*, **A32**, 751–767.
- Shapovalova M., Tolstykh N. and Bobrova O. (2019) Chemical composition and varieties of sulfosalts from gold mineralization in the Gaching ore occurrence (Maletoyvayam ore field). *IOP Conf. Series: Earth and Environmental Science*, **319**, 012019.
- Sidorov E.G., Borovikov A.A., Tolstykh N.D., Bukhanova D.S., Palyanova G.A. and Chubarov V.M. (2020) Gold mineralization at the Maletoyvayam deposit (Koryak Highland, Russia) and physicochemical conditions of its formation. *Minerals*, **10**, 1093.
- Škácha P., Buixaderas E., Plášil J., Sejkora J., Goliáš V. and Vlček V. (2014) Permingeatite, Cu_3SbSe_4 , from Příbram (Czech Republic): Description and Raman spectroscopy investigations of the luzonite-subgroup of minerals. *The Canadian Mineralogist*, **52**, 501–511.
- Škácha P., Sejkora J. and Plášil J. (2017) Selenide mineralization in the Příbram uranium and base-metal district (Czech Republic). *Minerals*, **7**, 91.
- Tolstykh N.D., Orsoev D.A., Krivenko A.P. and Izokh A.E. (2008) *Noble Metal Mineralization in Layered Ultramafic-basic Massifs in the South of the Siberian Platform*. Parallel Press, Novosibirsk, Russia, 194 pp. [in Russian].
- Tolstykh N., Sidorov E. and Kozlov A. (2009) Platinum group Minerals from the Olkhovaya-1 placer related to the Karaginsky ophiolite complex, the Kamchatskiy mys peninsula, Russia. *The Canadian Mineralogist*, **47**, 1057–1074.
- Tolstykh N., Vymazalová A., Tuhý M. and Shapovalova M. (2018) Conditions of Au–Se–Te mineralization in the Gaching ore occurrence (Maletoyvayam ore field), Kamchatka, Russia. *Mineralogical Magazine*, **82**, 649–674.
- Tolstykh N., Palyanova G., Bobrova O. and Sidorov E. (2019) Mustard gold of the Gaching ore deposit (Maletoyvayam ore Field, Kamchatka, Russia). *Minerals*, **9**, 489.
- Tolstykh N.D., Tuhý M., Vymazalová A., Plášil J., Laufek F., Kasatkin A.V., Nestola F. and Bobrova O.V. (2020) Maletoyvayamite, $Au_3Se_4Te_6$, a new mineral from Maletoyvayam deposit, Kamchatka peninsula, Russia. *Mineralogical Magazine*, **84**, 117–123.
- Tolstykh N., Bukhanova D., Shapovalova M., Borovikov A. and Podlipsky M. (2021) The gold mineralization of the Baranyevskoe Au–Ag epithermal deposit in Central Kamchatka. *Minerals*, **11**, 1225.
- Tolstykh N.D., Tuhý M., Vymazalová A., Laufek F., Plášil J. and Košek F. (2022) Gachingite, $Au(Te_{1-x}Se_x)_{0.2} \approx x \leq 0.5$, a new mineral from Maletoyvayam deposit, Kamchatka peninsula, Russia. *Mineralogical Magazine*, **86**, 205–213.
- Wang N. (2000) New synthetic ternary chalcogenides. *Neues Jahrbuch für Mineralogie*, **8**, 348–356.